E3S Web of Conferences 728, 01017 (2026)
EEUPD 2026
https://doi.org/10.1051/e3sconf/202672801017

Evaluation of the Emergency Response Capabilities for Flood Disasters in Shaanxi Province

Jing REN[1,2,*]

[1]College of Safety Science and Engineering, Xi'an University of Science and Technology, Xi'an 710054, China
[2]Xi'an Research institute of National Mine Rescue, Xi'an 710054, China

Abstract. With the rapid economic development and the frequent occurrence of extreme climate events, flood disasters pose an increasingly severe challenge to the safety of urban systems. To conduct scientific assessment and enhance the emergency response capabilities for flood disasters, First, analyze the causes and mechanisms of flood disasters. Based on the PSR theory, a multi-dimensional evaluation system consisting of 3 secondary indicators, 7 tertiary indicators, and 21 quaternary indicators is constructed. Ten prefecture-level cities in Shaanxi Province are selected as empirical objects, and official data from 2019 to 2023 are collected for quantitative assessment. Secondly, the entropy weight method and the coefficient of variation method are comprehensively applied to determine the weights of the indicators, and a comprehensive scoring model is constructed based on the weighted summation method. The spatial distribution map, dimension proportion map and time evolution map of the emergency response capability are drawn, and the evaluation grades of the flood disaster emergency response capabilities of each prefecture-level city are obtained. Finally, based on the analysis results, improvement paths are proposed. The results show that there are significant differences in the emergency response capabilities for flood disasters among various cities in Shaanxi Province. Among them, Xi'an City has an evaluation score of 0.5704, which is the highest; Yulin City follows closely with a score of 0.4631; in the southern part of Shaanxi Province, cities like Hanzhong and Weinan still need improvement. Tongchuan City has performed outstandingly in post-disaster recovery, while cities like Shangluo need to improve their level of early warning service information. This model provides a scientific basis for flood disaster emergency management, helping to reduce disaster losses and ensure the safety of people's lives and property.

1 Review

With global warming intensifying, sea levels are rising at an accelerated rate, and extreme weather events are occurring more frequently and with greater intensity. Climate change is posing increasing risks and challenges to humanity [1]. According to statistics from the Ministry of Emergency Management, the distribution of natural disasters shows clear regional differences, with northern regions more severely affected than southern ones. Taking 2023 as an example, economic losses caused by flood disasters accounted for 71.1% of all disaster-related losses. The frequent occurrence of flood disasters has had profound impacts on economic, social, and urban development, making them one of the most significant natural hazards [2]. To ensure sustainable urban development and safeguard the lives and property of residents, urban managers need to continuously monitor disaster risks and guide planning and policies to prevent the accumulation of risks [3]. Regular evaluation of emergency response capacity for flood disasters helps to understand the current level of preparedness, identify weak links, and formulate improvement measures [4].

Methods for assessing emergency response capacity to flood disasters can generally be divided into four categories: those based on historical disaster data [5], those based on remote sensing [6] and GIS technologies [7], those based on indicator systems [8], and those based on scenario simulation [9]. Historical disaster assessment methods require long-term data series and have difficulty fully capturing spatial variability [10]. Scenario simulation methods demand high data accuracy and involve high computational costs [11]. Remote sensing - based assessment methods are limited by accuracy constraints. Compared with the first three approaches, the indicator system - based method is grounded in the principles of natural disaster risk formation and analyzes disaster risk from both mechanistic and macro perspectives. By constructing an indicator system that reflects flood disaster risk, the assessment process is treated as a multi-objective decision-making problem [12]. At present, the development of flood disaster evaluation indicator systems has become relatively mature, with studies mainly focusing on three dimensions: risk assessment, loss assessment, and management assessment [13].

* Corresponding author: 2413651693@qq.com

Most scholars have extensively explored flood disasters from perspectives such as triggering mechanisms and influencing factors, achieving certain research outcomes. However, studies directly focusing on the evaluation of emergency response capacity for flood disasters remain relatively limited. In particular, there is a lack of research evaluating the comprehensive emergency response capacity of flood disasters. Therefore, taking Shaanxi Province as an example, this study compiles official data from 2019 to 2023, standardizes the data, and applies the entropy weight method and coefficient of variation method. Combined with the PSR theory, a flood disaster emergency response capacity evaluation model is constructed. Through analysis of spatial patterns and other aspects, the study aims to comprehensively grasp the overall characteristics of regional flood risk.

2 Emergency Response Capacity Evaluation Index System

2.1 Basis for Indicator Selection

2.1.1 Characteristics and Formation Mechanisms of Flood Disasters

With rapid economic development, extreme rainfall events caused by global climate change have become more frequent. Meanwhile, densely built high-rise buildings in cities hinder air circulation. In summer, heat emissions from building air-conditioning systems and vehicle exhaust are abnormally high, leading to the formation of thermal air currents. Over time, these hot air masses become increasingly dense, eventually triggering precipitation—a phenomenon known as the “rain island effect” [14]. Cities are often located in relatively low-lying and flat areas, making them prone to receiving inflow from surrounding regions while possessing weak natural drainage capacity. Additionally, human activities have widely covered the ground surface with impermeable layers, disrupting the natural hydrological cycle. Rainwater is unable to infiltrate into the ground, resulting in severely insufficient flood discharge capacity [15].

Accumulated rainwater cannot be effectively drained through natural channels and must rely on drainage pipe networks for forced discharge. During urban construction, emphasis is often placed on above-ground development, while underground infrastructure receives insufficient attention. This leads to relatively low standards for drainage and flood discharge facilities [16]. When regional flooding occurs, inadequate drainage systems struggle to cope with large volumes of urban runoff, exacerbating waterlogging depth and prolonging its duration. As a result, the spatial extent and impact of flood disasters continue to expand, while the likelihood of secondary disasters increases, severely affecting residents’ quality of life and urban infrastructure.

2.1.2 Theoretical Framework for Evaluating Flood Disaster Emergency Response Capacity

The Pressure-State-Response theory was first proposed in 1979 by Canadian statisticians David J. Rapport and Tony Friend [17]. It has since been widely applied in fields such as water environmental safety assessment and environmental impact assessment in urban planning. Furthermore, with the deepening understanding of disaster risks, PSR theory has also been used in disaster risk assessments of protected areas, as well as in evaluations of regional ecological security and ecological risks involving ecosystems and geomorphological types [18].

This model framework clearly explains the chain of interactions among driving forces, internal system states, and human activities within urban human－land coupled systems. It allows for the construction of a single-disaster risk assessment index system from three perspectives: pressure inputs faced by the system, changes in the system’s internal state, and feedback responses of the system [19].

Based on the PSR model, and in combination with the mechanisms of flood disaster formation and practical urban governance, a multi-dimensional approach is adopted, incorporating factors such as the natural environment and social structure, as shown in Fig. 1.

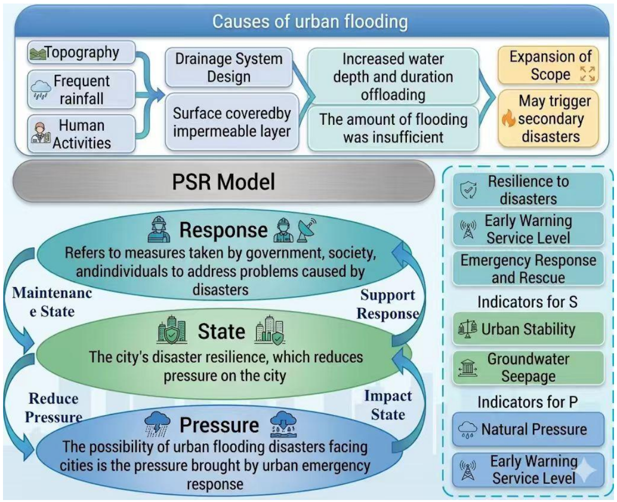

Fig. 1. Theoretical framework for evaluating flood disaster emergency response capabilities based on PSR theory.

2.2 Construction of the Evaluation Index System

By analyzing the formation mechanisms of flood disasters and integrating the PSR theory, this study examines the influencing factors of emergency response capacity to flood disasters. Using the literature review method, relevant research findings were compiled, and key studies were screened and analyzed to construct an evaluation index system. This system consists of three secondary indicators (Pressure－State－Response), seven tertiary indicators, and twenty-one quaternary indicators, as shown in Fig. 2. Among them, indicators R2 to R4 are negative indicators, while the rest are positive indicators.

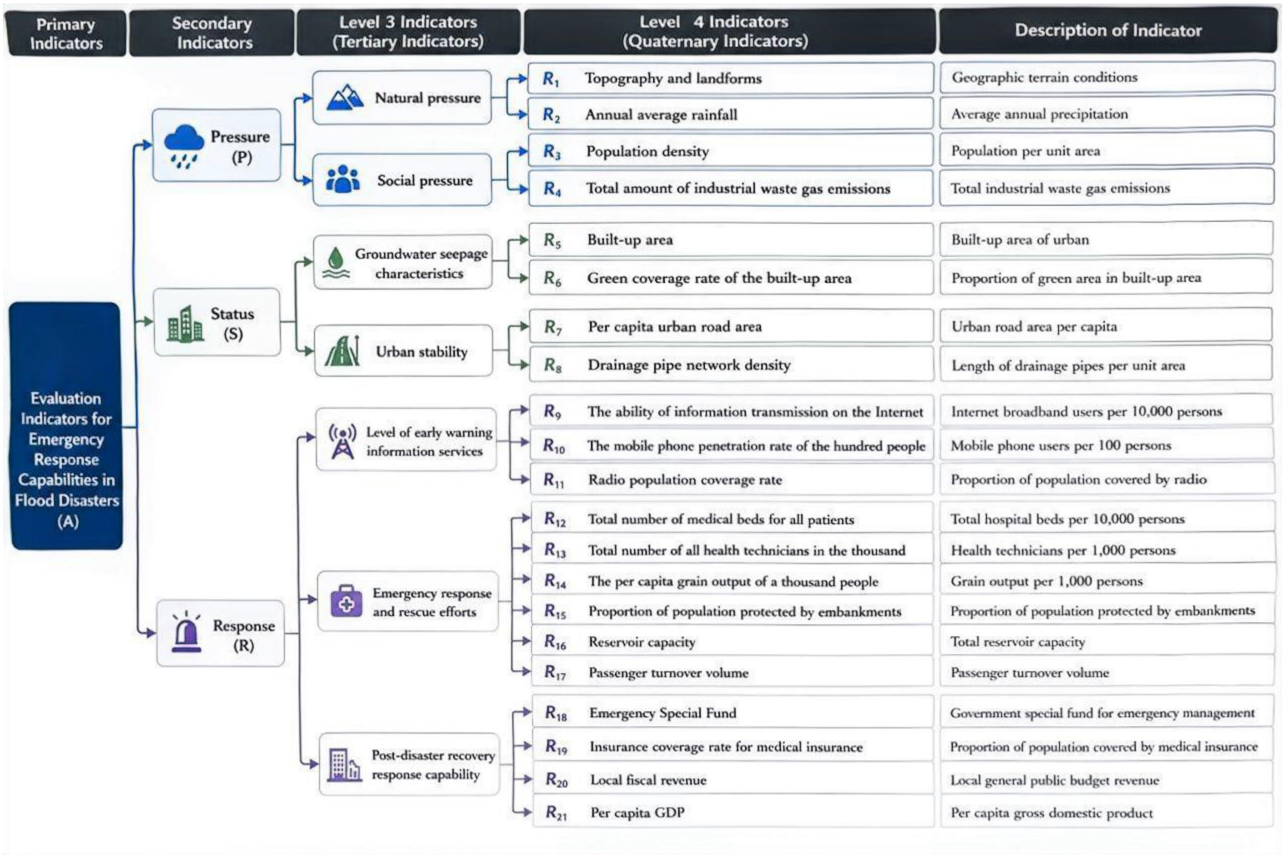

Fig.2 Flood disaster evaluation index system

2.3 Overview of the Study Area

Shaanxi Province is geographically located between 105°29′–111°15′ E longitude and 31°42′–39°35′ N latitude. Due to the natural boundary formed by the Qinling Mountains and the Huaihe River, the province spans both northern and southern China. The river systems in Shaanxi mainly belong to the Yellow River and Yangtze River basins, as shown in Fig. 3. The Yellow River basin within Shaanxi covers approximately 133,300 square kilometers, accounting for 64.7% of the province's total area. Major tributaries in Shaanxi include the Kuye River, Wuding River, and Yan River.

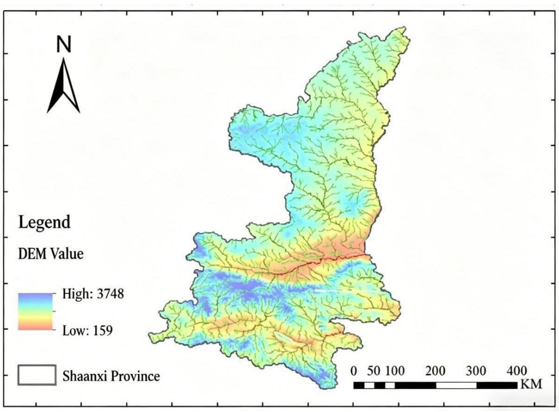

Fig.3 Research on the overview of the river system in the study area

The natural geographical characteristics of Shaanxi make it particularly susceptible to flood disasters. During the rainy season, terrain conditions often lead to short-duration intense rainfall, causing rapid river swelling and flash floods, especially in southern Shaanxi, in basins such as the Han River and Jialing River. Flood disasters not only threaten the safety of lives and property but also severely impact local agriculture, transportation, and urban infrastructure.

3 Emergency Response Capability Evaluation Model

3.1 Data Sources

We collected and compiled statistical annuals, statistical bulletins, and other official publications issued by the Ministry of Housing and Urban-Rural Development of the People's Republic of China, the Shaanxi Provincial Bureau of Statistics, and various municipal governments from 2020 to 2024. We obtained official data on relevant indicators for the period from 2019 to 2023. For the missing values present in the dataset, we employed the Stata linear interpolation method to handle the missing values in a scientific and reasonable manner. This method uses a local linear assumption to fill in the missing data with certainty. During the data collection process, a small number of missing values were identified in indicators such as drainage pipe density for certain cities mainly in 2020–2021. The proportion of missing data was less than 2% of the total dataset.

To ensure data continuity, linear interpolation in Stata was applied. To assess the robustness of the results, a sensitivity check was conducted by comparing the rankings before and after interpolation. The results show that the interpolation had no significant impact on the overall ranking of cities, indicating that the evaluation results are relatively stable and reliable.

The terrain and landform characteristic indicators within the stress layer (R1) are obtained by combining the elevation, slope, and slope orientation of the study area. These three factors are the most common indicators that reflect the micro-characteristics of the ground surface. First, image data for Shaanxi Province were downloaded from the GeoSpatial Data Cloud website, and a high-resolution elevation map of Shaanxi Province was obtained. Using raster attributes, the average elevation was calculated to represent the average height of the surface within the region. Subsequently, the Spatial Analyst tool in ArcGIS was used for surface analysis, extracting data on slope and slope orientation, and calculating the average slope and slope orientation of the study area to reflect the level of undulation in the ground surface. Finally, the average elevation, slope, and slope orientation were combined to obtain the corresponding values for each prefecture-level city in Shaanxi Province. Fig. 4 provides an example of the terrain and landform analysis results for Xi’an City. Similar operations can be performed for the other nine prefecture-level cities to obtain the required indicator data.

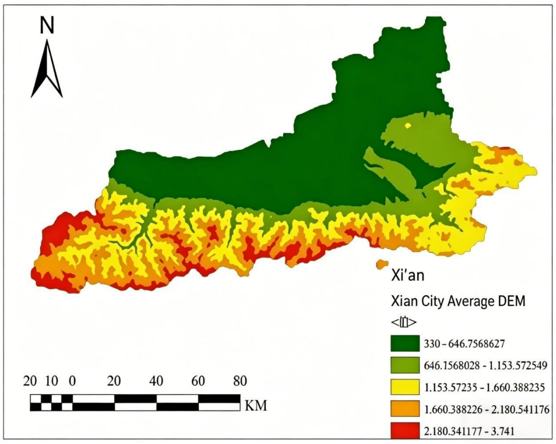

(a) Results of Xi’an’s Elevation Analysis

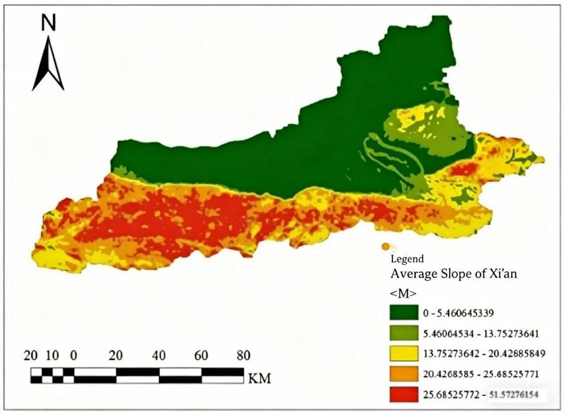

(b) Results of slope analysis for Xi’ an City

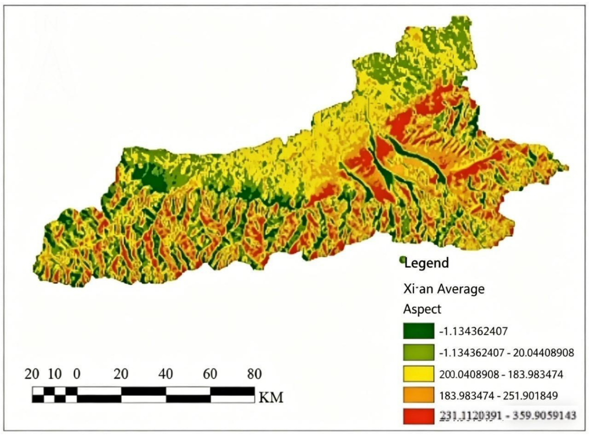

(c) Analysis results of slope orientation in Xi’ an City

Fig.4 GIS extraction results of topographical analysis (Xi'an City as an example)

3.2 Data standardization

In the field of thermodynamics in physics, entropy is a concept used to describe the state of disorder in a system. Shannon built upon this concept and, in his pioneering paper, developed information theory, introducing information entropy to quantify the uncertainty or degree of disorder associated with information. In multi-criteria decision analysis, the entropy weight method utilizes the principles of information entropy to assess the impact of changes in various indicators on the overall system[20]. This method determines weights by analyzing the variability of indicator values, but it may overlook overall balance by focusing solely on the changes in information between indicators, resulting in an uneven distribution of weights. The variance coefficient method focuses on the relative fluctuations of indicator values within a evaluation system. It measures and compares the differences between different evaluation objects by calculating the variance coefficient of the indicators. This approach can highlight the differences between indicators and, to some extent, compensate for the shortcomings of the entropy weight method in terms of balance[21].

Based on this, in order to reduce subjective randomness and the uncertainty introduced by a single method, a comprehensive weight determination method that combines entropy weighting and variance coefficient methods was proposed. This integrated approach aims to balance the strengths of both methods, thereby enhancing the objectivity and accuracy of weight allocation, thus providing a more robust weight configuration for multi-indicator comprehensive evaluation.

$$R=\begin{bmatrix} r_{11} & r_{12} & \cdots & r_{1n} \\ r_{21} & r_{22} & \cdots & r_{2n} \\ \vdots & \vdots & \ddots & \vdots \\ r_{m1} & r_{m2} & \cdots & r_{mn} \end{bmatrix} \tag{1}$$

Linear transformations are used to eliminate differences in units between the data, allowing all indicators to be compared on the same scale. Positive indicators are those where higher values indicate better evaluation outcomes, while negative indicators are the opposite, with lower values indicating better evaluation outcomes. The calculation steps are as follows.

Positive indicator.

$$R_{ij}=\frac{r_{ij}-r_{\min}}{r_{\max}-r_{\min}} \tag{2}$$

Negative indicator.

$$R_{ij}=\frac{r_{\max}-r_{ij}}{r_{\max}-r_{\min}} \tag{3}$$

After undergoing standardization processing, a standardized matrix is obtained.

$$R_{ij}=\begin{bmatrix} R_{11} & R_{12} & \cdots & R_{1n} \\ R_{21} & R_{21} & \cdots & R_{2n} \\ \vdots & \vdots & \ddots & \vdots \\ R_{m1} & R_{m2} & \cdots & R_{mn} \end{bmatrix} \tag{4}$$

3.3 Variance coefficient method

The basic idea of the variance coefficient method is to use the degree of variation in the data to determine the weights of the indicators. The core of this method is the notion that indicators with greater variation carry more information. The calculation steps are as follows.

Calculate the average value for each indicator.

$$\overline{R_j}=\frac{1}{n}\sum_{j=1}^{n}R_{ij} \tag{5}$$

Calculate the standard deviation for each indicator.

$$\partial_i=\frac{\sqrt{\sum_{j=1}^{n}\left(R_{ij}-\overline{R_j}\right)^2}}{n} \tag{6}$$

Calculate the coefficient of variation for the indicator.

$$V_j=\frac{\partial_j}{R_j} \tag{7}$$

Determine the weights of the indicators.

$$W_{j1}=\frac{V_j}{\sum_{j=1}^{n}V_j} \tag{8}$$

3.4 Entropy weighting method

Using an index matrix, standardize the data, and then employ the entropy weight method to calculate the information entropy of each indicator. Use normalized values to compute the information entropy of the jth index, and subsequently determine the weights. The calculation was performed as follows.

Calculate the entropy value for the j-th indicator.

$$E_j=-\frac{1}{\ln m}\sum_{i=1}^{m}\frac{R_{ij}}{\sum_{i=1}^{m}R_{ij}}\ln\frac{R_{ij}}{\sum_{i=1}^{m}R_{ij}} \tag{9}$$

Information utility value.

$$d_j=1-E_j \tag{10}$$

Calculate the entropy weights for an indicator.

$$W_{j2}=\frac{1-E_j}{\sum_{j=1}^{n}\left(1-E_j\right)} \tag{11}$$

3.5 Emergency response capability rating.

Refer to LI’s research[22]. The relative importance of the two weights is determined by setting a composite allocation preference coefficient. In this study, the composite allocation preference coefficient was set to 0.5, indicating that the variance coefficient method and the entropy weight method were given equal importance. The calculation steps are as follows.

$$W_j=\lambda\times W_{j1}+(1-\lambda)\times W_{j2} \tag{12}$$

Finally, in order to comprehensively evaluate the capabilities of various prefectures in responding to flood disasters, a weighted summation and averaging method was employed. The calculation steps are as follows.

$$A=\sum_{j=1}^{n}W_j\times R_{ij} \tag{13}$$

4 Case application and analysis

4.1 Spatial pattern

Fig. 5 shows the spatial distribution of emergency response capabilities in 10 cities of Shaanxi Province. From the pressure layer distribution in Fig. 5 (a), the scores present a pattern of high in the periphery and general in the central part. The cities in the central part of Shaanxi Province, such as Xi'an, Xianyang and Weinan, show relatively high pressure levels, facing significant social and economic development pressure as well as resource and environmental burdens. The pressure levels in the peripheral areas of Shaanxi Province, such as Yulin and Ankang, are relatively lower, with values higher than 0.27, and the impact of development activities on the environmental system is relatively smaller.

From the state layer distribution in Fig. 5(b), it can be seen that the state values of Xi'an City and Yulin City are relatively high, indicating that the drainage capacity of the urban areas is strong, the natural hydrological system is relatively intact, and the disaster resilience is strong. This can alleviate the pressure brought by flood disasters. In contrast, the state layers of cities such as Xianyang City, Ankang City, and Yan'an City need to be improved.

Fig. 5(c) shows the distribution of response levels. Regions such as Xi'an, Yulin, and Ankang have relatively high response values, indicating that they have a good emergency response capability and can mitigate the losses caused by disasters; while the response levels in cities like Shangluo and Weinan need to be improved.

Based on the Flood Disaster Emergency Response Capability Evaluation Model, the final level of emergency response capability for each prefecture-level city in Shaanxi Province can be obtained. The final emergency response capability level is derived from the mean of scores from 2019 to 2023. Geographic Information System (GIS) technology using Jenks natural break classification method was employed to grade the prefecture-level cities in Shaanxi Province, categorizing their emergency response capabilities into four levels: high, higher, medium, and general. The results of the grading are shown in Table 1, and the spatial distribution of emergency response capabilities is depicted in Figure 5(d). Different shades of green represent different levels of urban emergency response capabilities, and the green color gradually becomes lighter from deep to indicate the decreasing level of urban flood resilience.

Table 1 Classification results of natural breakpoint classification method

level	Section
high	0.330001—0.520000
higher	0.270001—0.330000
medium	0.180001—0.270000
general	0.180000

Among the 10 prefecture-level cities in Shaanxi Province, the emergency response capabilities of Xi'an City and Yulin City are at a high level, while those of Yan'an City, Baoji City, Tongchuan City and Ankang City are at a relatively high level, those of Xianyang City, Hanzhong City and Shangluo City are at a medium level, and Weinan City is at a general level.

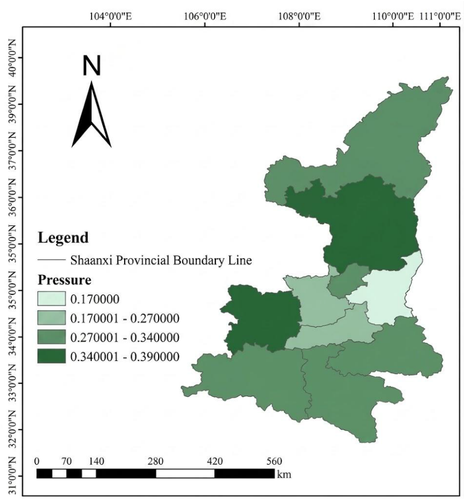

(a) Analysis of the pressure layer.

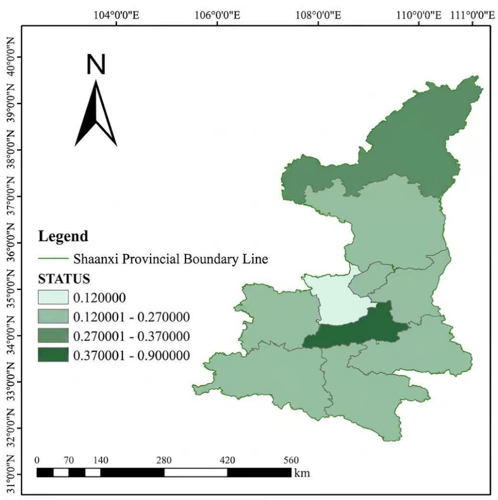

(b) Analysis of the state layer.

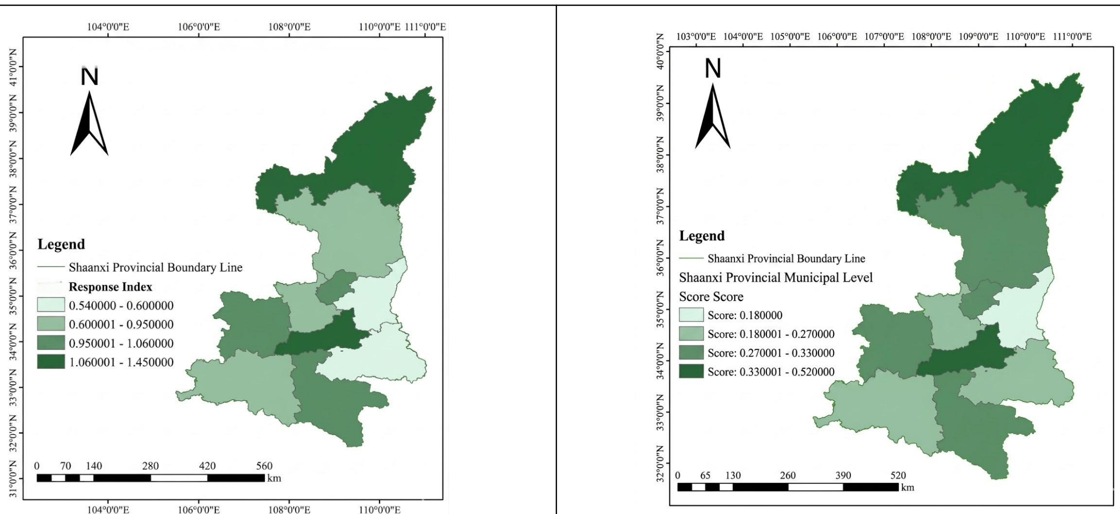

(c) Layer-wise analysis. (d) Emergency response capabilities

Fig.5 Spatial distribution of emergency response capabilities

4.2 Dimensional analysis

Based on the proportion of each dimension of emergency response capability, Fig. 6 shows the proportion of emergency response capability dimensions, covering 8 core capability dimensions of 10 prefecture-level cities. By analyzing the proportion differences of the capability structures of each city, it is possible to directly identify the dimensions that each city can improve.

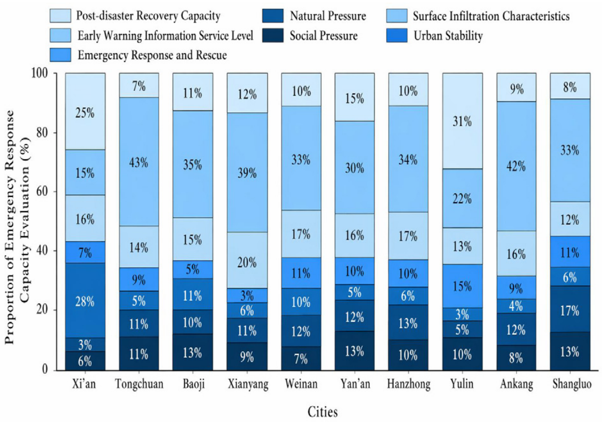

Fig.6 Proportion of emergency response capability dimension

The proportion of natural pressure in Xi'an is 6%, while the proportion of the social pressure dimension is only 3%. Both of these proportions are at the bottom of the province. Xi'an is facing significant natural pressure and development pressure. The natural pressure is reflected in natural factors such as complex terrain and frequent extreme precipitation, while the development pressure is reflected in population density growth. Yulin City only has a 5% proportion of the social pressure dimension, which is reflected in the total amount of industrial waste gas emissions.

The weights of the two dimensions - ground water seepage characteristics and urban stability - account for less than 20% in most cities. The combined proportion of the status layer indicators in Xianyang City and Ankang City is at the bottom of the province, indicating that there is still considerable room for improvement in aspects such as drainage system layout and drainage efficiency.

In the emergency response and rescue aspect, the proportions in cities such as Tongchuan, Ankang, Xianyang, and Shangluo all exceeded 30%. Among them, Tongchuan reached 43%, which was the highest in the province, indicating that in most cities, the post-disaster remediation and recovery mechanisms are relatively complete and possess strong post-event response capabilities. In terms of the level of early warning information services and emergency response and rescue, the proportions in some cities were still relatively small, and there is still room for improvement in emergency preparedness, collaborative coordination, and information system construction.

4.3 Temporal analysis

The changes in the pressure layer scores of each city in Shaanxi Province from 2019 to 2023 are shown in Fig. 7(a). In the pressure layer, the indicators related to terrain and topography have basically not undergone significant changes in recent years, and their influence on the trend of pressure layer changes can be disregarded; the pressure layer scores of Baoji City and Yulin City have relatively stable changes, and the changes in population density and industrial waste gas emissions are small; in 2021, the scores of most cities in Shaanxi Province generally showed a downward trend, except for Yulin City, the other 9 cities all reached the lowest values in the past five years, indicating that the region is under significant pressure. The phenomenon of the overall decline in the provincial score is mainly due to the abnormal increase in the annual precipitation within the province in 2021, which led to a greater natural pressure on cities before natural disasters occurred. During the period from 2022 to 2023, the pressure layer scores of Tongchuan City, Xi'an City, Ankang City, and other places showed a downward trend, which is related to urban economic development, and the industrial waste gas emissions increased. Among them, Xi'an has also been affected by the combined effect of population inflow, resulting in significant social pressure on the city.

The changes in the status layer scores of all cities in Shaanxi Province from 2019 to 2023 are shown in Fig. 7(b). The scores at this level generally showed an upward trend. This indicates that during the evaluation period, most cities in Shaanxi Province made significant progress in urban construction and infrastructure. Xi'an, as the provincial capital of Shaanxi Province, benefited from its abundant resources and administrative advantages, and its score was ahead of other cities. Its built-up area, built-up area green coverage rate, and per capita urban road area were all higher than those of other cities. Yan'an City focused on underground drainage pipe construction from 2019 to 2020, and the density of drainage official networks significantly increased. The built-up area green coverage rate and per capita urban road area also steadily increased, and its status layer score significantly increased, with a change rate of 116%. Tongchuan City, Baoji City, Ankang City, and other cities had relatively small fluctuations in their scores, but the overall trend was positive.

The changes in the response layer scores of all prefecture-level cities in Shaanxi Province from 2019 to 2023 are shown in Fig. 7(c). All prefecture-level cities in Shaanxi Province generally showed a growth trend. In particular, Xi'an City and Yulin City were significantly ahead of other cities in terms of emergency response capabilities. During the evaluation period, Xi'an City's overall scores in multiple dimensions such as early warning information service level, emergency response and rescue were consistently higher than those of other prefecture-level cities, and showed a stable growth trend, indicating that it has achieved remarkable results in the construction of the emergency response system. Yulin City mainly benefited from its relatively high per capita GDP and sufficient emergency funds. The emergency response capabilities of Tongchuan City, Shangluo City, Yan'an City and other cities also showed a growth trend.

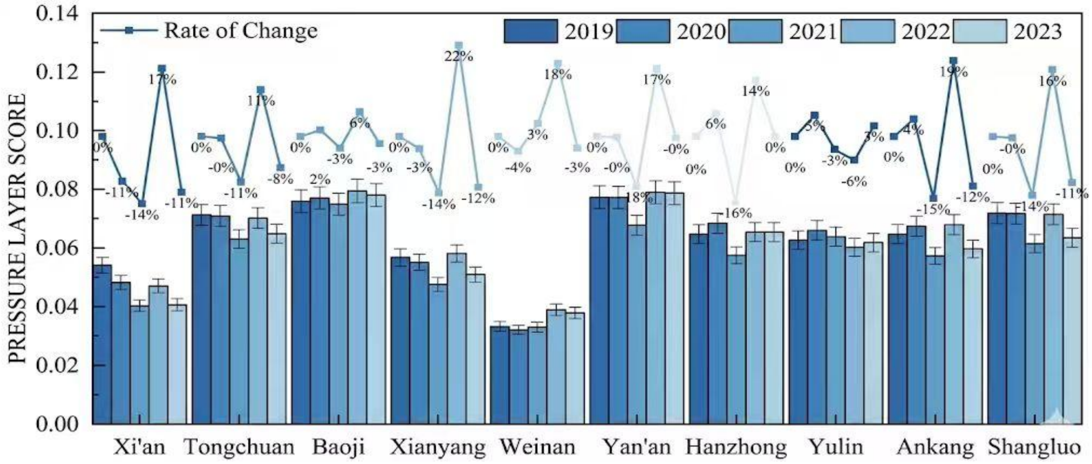

(a) Pressure Layer

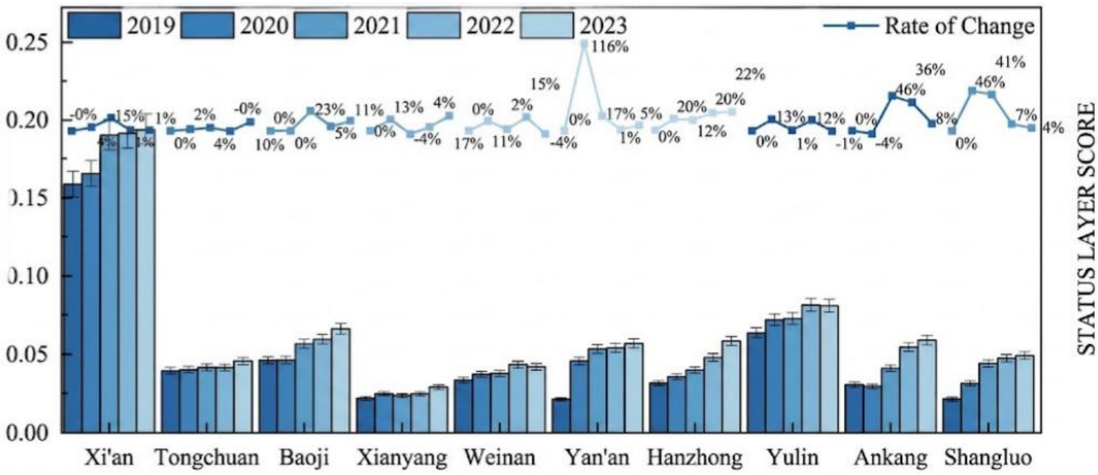

(b) State Layer

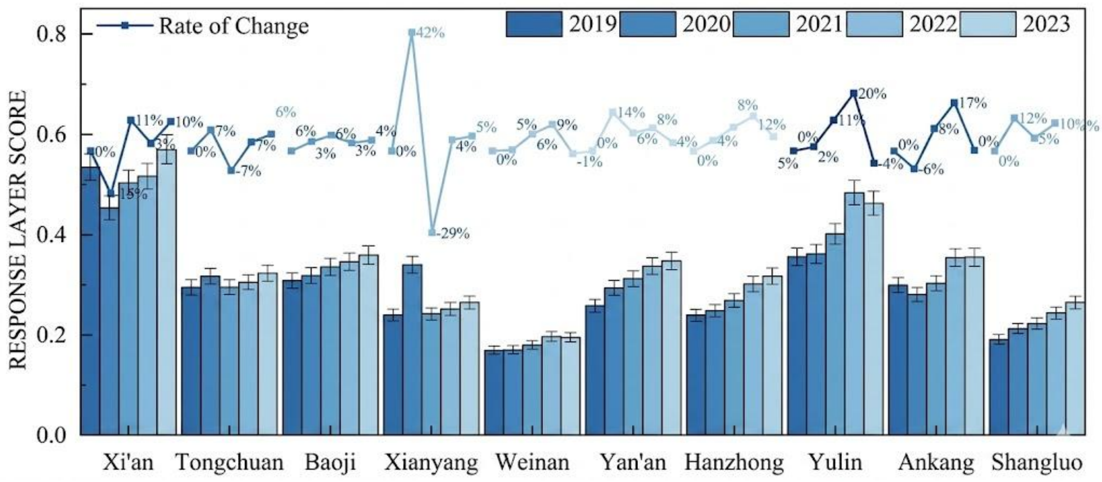

(c) Response Layer

Fig.7 Temporal evolution of emergency response capabilities

5 Conclusion

(1) There is a significant difference in overall levels. The differences among cities in Shaanxi Province are notable. Xi'an and Yulin have the highest scores and demonstrate a strong comprehensive emergency response capability; Yan'an, Baoji, Tongchuan, and Ankang are at a relatively high level; Xianyang, Hanzhong, and Shangluo are at a medium level; and Weinan has an overall level that is at a general level.

(2) The spatial layout exhibits differentiated characteristics. Xi'an, the provincial capital, has a relatively complete infrastructure and resource allocation, and thus ranks first in the overall score across the province; Yulin City, relying on a relatively high level of economic development and fiscal investment, has a strong ability to respond and recover; Tongchuan City has a prominent advantage in post-disaster recovery; while Weinan and Shangluo regions need to improve in terms of early warning information services, drainage systems, and social adaptability. Overall, the pattern is characterized as "better in the Guanzhong region and weaker in the Shaanxi southern region".

(3) Dimensional differences reveal improvement in dimensions. The overall trend at the status layer is upward, indicating that most cities have made progress in infrastructure and green space construction. However, cities like Xianyang and Ankang still need to improve in terms of drainage systems and urban stability. The response layer contributes the most to the comprehensive capabilities. Tongchuan and Ankang have outstanding performances in emergency response and rescue dimensions. However, the proportion of the early warning information service system in multiple cities is relatively general, and there is insufficient informatization and public participation.

(4) The temporal evolution shows a trend of stability with an increase. From 2019 to 2023, all cities generally showed a gradual upward trend. Among them, Xi'an and Yulin maintained the leading position and had stable growth; Yan'an saw significant improvement in its state layer indicators due to increased investment in pipeline construction; however, in 2021, extreme precipitation events caused a sharp drop in the pressure layer scores of most cities.

The research has achieved certain results in the construction of the index system and the application of the model, but there are still deficiencies. Future research can strengthen the acquisition and integration of multi-source high-resolution data, and improve the refinement and dynamicization level of the index system; introduce multi-disaster coupling risk assessment methods to construct a comprehensive emergency response model that better suits the actual situation of the region; combine time series prediction models or artificial intelligence methods to conduct trend prediction and dynamic evolution analysis of the city's emergency response capability.

References

1. NING Shiqiang, GAO Guoping, LI Xiaoyan, et al., Journal of Xi'an University of Science and Technology 42, 1264-1271 (2022). https://doi.org/10.13800/j.cnki.xakjdxxb.2022.0625.
2. Office of the National Disaster Reduction Committee, Ministry of Emergency Management, China Disaster Reduction 3, 7 (2024). https://www.mem.gov.cn:10443/xw/yjglbgzdt/202401/t20240120_475697.shtml
3. WANG H, YE H, LIU L, et al., International Journal of Environmental Research and Public Health 19, 10200 (2022). https://doi.org/10.3390/ijerph191610200.
4. KROGH A H, ROISELAND A, Journal of Homeland Security and Emergency Management 21, 27-47 (2024). https://doi.org/10.1515/jhsem-2022-0005.
5. LUO Zhenmin, SHEN Jiatong, PAN Jingchao, et al., Journal of Xi'an University of Science and

Technology 45, 845-854 (2025). https://doi.org/10.13800/j.cnki.xakjdxxb.2025.0501.

6. GHAFFARIAN S, KERLE N, FILATOVA T, Remote Sensing 10, 1760 (2018). https://doi.org/10.3390/rs10111760.
7. Ahsen Maqsoom;Bilal Aslam,etal., Modeling Earth Systems and Environment 2, 1519-1533 (2022). https://doi.org/10.1007/s40808-021-01226-0.
8. DONG Shuchang, MA Donghui, ZHANG Boqian, et al., Journal of Disaster Prevention and Mitigation Engineering 44, 762-771, 808 (2024). https://doi.org/10.13409/j.cnki.jdpme.20230831002.
9. QUAN R, Arabian Journal of Geosciences 14, 943 (2021). https://doi.org/10.1007/s12517-021-07345-3.
10. XU H, MA C, LIAN J, et al., Journal of Hydrology 563, 975-986 (2018). https://doi.org/10.1016/j.jhydrol.2018.06.060.
11. GRIMALDI S, SCHUMANN G J P, SHOKRI A, et al., Water Resources Research 55, 5277-5300 (2019). https://doi.org/10.1029/2018WR024289.
12. GUAN X, LIU Y, MENG Y, et al., Water Resources Management 39, 1521-1549 (2025). https://doi.org/10.1007/s11269-024-04035-z.
13. XU Z, CHEN H, REN M, et al., Advances in Water Science 31, 713-724 (2020). DOI: 10.14042/j.cnki.32.1309.2020.05.008.
14. HU Caikong, LIU Chengshuai, LI Xiang, et al., Water Resources Protection 39, 152-159 (2023). DOI:10.3880/j. issn.1004 - 6933.2023.02.019.
15. GU Hongbo, GU Jian, Journal of Shanxi Agricultural University (Social Science Edition) 11, 1164-1169 (2012). https://doi.org/10.13842/j.cnki.issn1671-816x.2012.11.001.
16. ZHANG Yihang, WEN He, ZHENG Dan, Building Structure 50, 138-141, 113 (2020). https://doi.org/10.19701/j.jzjg.2020.23.024.
17. VAN S N, RONSYN J, WILLEMS P, Environmental Modelling & Software 33, 92-105 (2012). https://doi.org/10.1016/j.envsoft.2012.01.013.
18. YANG Qin, KE Yinghai, LI Xiaojuan, et al., Journal of Henan Polytechnic University (Natural Science) 37, 79-85 (2018). https://doi.org/10.16186/j.cnki.1673-9787.2018.03.11.
19. YANG Haifeng, ZHAI Guofang, Journal of Natural Resources 36, 2368-2381 (2021). https://doi.org/10.31497/zrzyxb.20210914.
20. SU Yongwei, CHEN Chibo, Statistics & Decision 35, 38-41 (2019). https://doi.org/10.13546/j.cnki.tjyjc.2019.24.008.
21. ZHU Y, TIAN D, YAN F, Mathematical Problems in Engineering 2020, 3564835 (2020). https://doi.org/10.1155/2020/3564835.
22. CHEN L, HUO C, Sustainability 14, 9293 (2022). https://doi.org/10.3390/su14159293.